

Ozgu Kasmer
Resat Ulusay
Candan Gokceoglu

Spoil pile instabilities with reference to a strip coal mine in Turkey: mechanisms and assessment of deformations

Received: 3 June 2005
Accepted: 23 August 2005
Published online: 29 November 2005
© Springer-Verlag 2005

Abstract With the increasing adoption of the surface mining of coal, problems associated with spoil pile instability, which affects resource recovery, mining cost, and safety and presents environmental hazards, have become a matter of prime concern to mine planners and operators. The study of geotechnical aspects is thus very important in the rational planning for the disposal, reclamation, treatment and utilization of spoil material. A strip coal mine, one of the largest open pit mines in Turkey, is located in Central Anatolia and provides coal to a thermal power station. Coal production is carried out in two adjacent open pits, the Central Pit and South Pit. A large-scale spoil pile instability over an area of 0.3 km² occurred within the dumping area of the Central pit. In addition, small-scale movement occurred in the outside dumping area. This paper outlines the results of field and laboratory investigations to describe the mechanisms of the spoil pile instabilities and to assess deformations monitored over a long period following the failure. Shear test results indicate that the interface between the floor and spoil material dumped by dragline has a negligible

cohesion and is the most critical plane of weakness for spoil pile instability. Back analyses based on the method of limit equilibrium and the numerical modelling technique, and observations in the pit revealed that failure occurred along a combined sliding surface consisting of a circular surface through the spoil material itself and a planar surface passing along the interface between the spoil piles and floor. The analyses also indicated that pore water pressure ratios of about 0.25 satisfy limiting equilibrium condition and that rainfall about one month before the failure may be a contributing factor to the instability. Movement monitoring data obtained following the failure over a 1.5-year period suggested that the ongoing deformations were mainly due to compaction of the spoil material. Based on the monitoring data and the results of the analyses, the failure mode of the local instability occurring at the outside dumping area was considerably similar to that of the large instability.

Keywords Combined failure · Finite element method · Movement monitoring · Open pit · Shear strength · Spoil pile instability

O. Kasmer · R. Ulusay (✉)
C. Gokceoglu
Geological Engineering Department,
Hacettepe University, 06532 Beytepe,
Ankara, Turkey
E-mail: resat@hacettepe.edu.tr
Tel.: +90-312-2977767
Fax: +90-312-2992034

Introduction

In most open pits throughout the world, overburden is disposed of in dumping areas. Due to blasting, excavation and transportation, the overburden breaks down into smaller particles. Additionally, traffic loads and atmospheric effects accelerate the degradation of spoil material. Coal mine waste material, which usually consists of a mixture of coarse-grained particles to rock

fragments grading to fine-grained material, causes problems due to spoil pile failures. Aside from environmental considerations, these failures affect resource recovery, mine safety and mining costs. There exist many examples of spoil instabilities that have resulted in loss of life and/or damage to property, and interruption in production (i.e. Bowman and Gilchrist 1978; Richards et al. 1981; Okagbue 1987; Speck et al. 1993; Ulusay et al. 1995). These large-scale failures and their

drastic consequences focused the attention of engineers on the importance of the stability of spoil piles, as much as highwall stability, in open pit mining.

Surface mining activities associated with the production of coal are increasing in Turkey, particularly for use in thermal power stations. One of the largest open pit coal mines in Turkey is located in Central Anatolia and produces coal for a thermal power station with a capacity of 300 MW. It has been in production since 1988 supplying 3.8 million tonnes of lignite per annum. Coal production is carried out at two adjacent open pits, called the “Central Pit” and “South Pit”. No instability problem was experienced in either the pit slopes or the spoil piles until 2001. Following an unexpected rainfall event in May 2001, a large-scale spoil pile failure (labeled INS1) occurred in June 2001 in the inside dumping area and the spoil material moved towards the highwall of the Central Pit over a distance of 600 m in NNW direction (Fig. 1a). In addition, a small-scale local instability (labeled INS2) also occurred in the old outside dumping area that was left years ago (Fig. 1b), but it did not affect mining operations.

The objective of this study is to describe both spoil pile failures mentioned above, the nature of movements,

and the possible failure mechanisms to evaluate the parameters of the materials involved, and to discuss how these factors could have influenced the spoil pile stability. Prime consideration was given to assessing the failure mechanisms, the behavior of the floor material and possible triggering factors. To accomplish this task, observations, post-failure topographical surveys, groundwater considerations, movement monitoring and geomechanical laboratory testing were used in conjunction with back-analyses of the spoil failures. The two-dimensional limit equilibrium method of analyses and finite element method (FEM) were used to assess the failure mechanisms and the various controls on slope stability.

Site description

Current mining practice

Coal production at the investigated mine is carried out at two adjacent open pits called the “Central Pit” and the “South Pit”, respectively (Fig. 2). All of the coal currently being produced is won from two coal seams

Fig. 1 Panoramas showing the spoil pile instabilities labeled INS1 in the Central Pit (a), and INS2 at the outside dumping area (b)

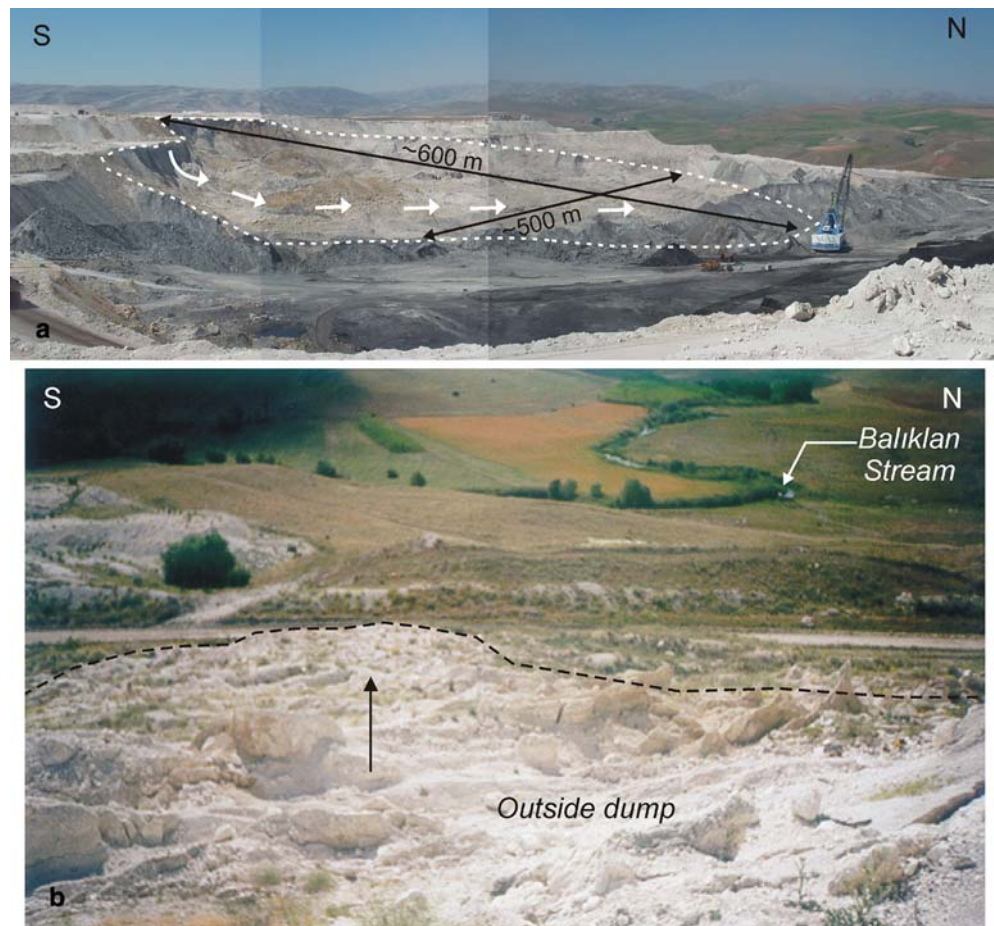
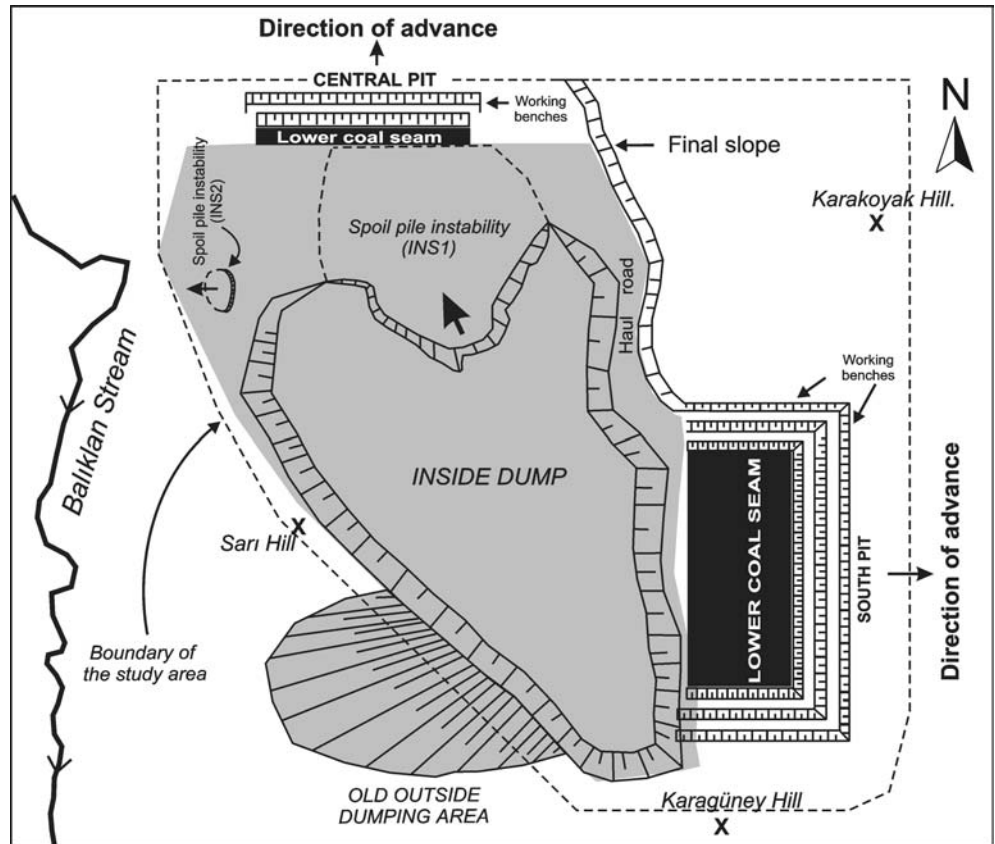


Fig. 2 Simplified layout plan of the open pits and dumping areas, and locations of the spoil pile instabilities



with an average thickness of 7 m in both pits by the strip mining method. There is an interburden 20 m thick between the upper and lower coal seams and this is mined by a walking dragline (a Marion 8050 with a 99 m boom and 50 m³ bucket; Fig. 3). The dragline dumps the interburden into the void about 45 m behind the working face to form dragline spoil piles about 30 m high. Electrically operated excavators with a 15 m³ bucket capacity excavate the overburden, which is approximately 80 m thick, and form pit benches 14 m high. Both coal seams are excavated by excavators. Coal produced from both seams is mixed in order to obtain an optimum calorific value, and delivered to the power station. A light blast is used to loosen the limestones at the uppermost benches. Mining activity in the Central Pit has been initiated at the east of Sari Hill and the current direction of advance is towards the north. The N–S oriented South Pit advances to the east (see Fig. 2). When mining began in the Central Pit, spoil material was dumped in the outside dumping area located on natural slopes dipping towards the Baliklan Stream to the west (see Fig. 3). This area was left after the outside dumping was completed, then reclaimed. Currently, there is no need for an outside dumping area. Spoil piles in the inside dumping area were normally constructed at their angle of repose of 35° in an E–W direction. The direction of mining advance was down dip until spoil

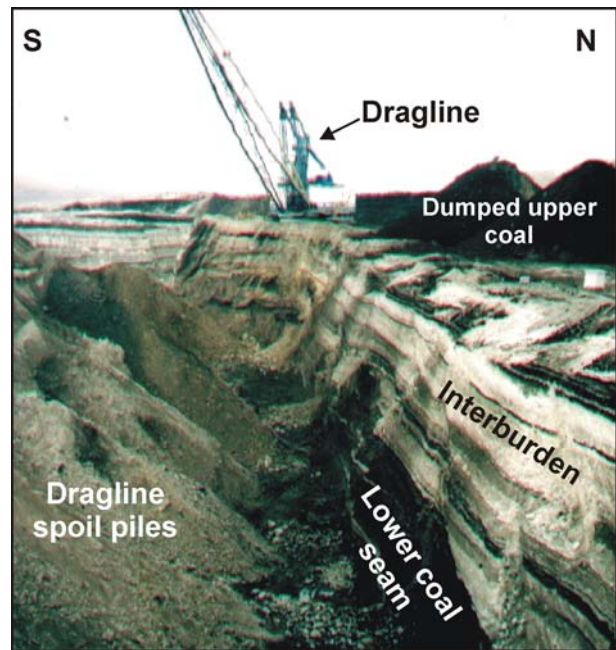


Fig. 3 Panorama illustrating the stripping operation by the dragline in the Central Pit

failure INS1 occurred in the Central Pit. Therefore, the dragline dumped the spoil piles up-dip onto the bottom clay. The total height of the dumps consisting of a number of benches was 115 m.

Geology

The Tertiary coal measures overlie Jurassic-Cretaceous aged re-crystallized limestones and ophiolitic rocks, and comprise the Kalburcayiri and Bicir formations. Plio-Quaternary aged young basalts and Quaternary alluvial deposits overlie these rock units (Fig. 3).

Based on borehole data obtained by the Mineral Research and Exploration Institute (MTA) of Turkey (MTA 1976), the thickness of the Kalburcayiri formation reaches up to 130 m. A sequence composed of conglomerates, including limestone-originated gravels within carbonate cement, represents the bottom of this formation, and it does not outcrop in the pit or its vicinity. Grayish-green, firm to stiff and generally massive silty clay overlies the basement conglomerates. Horizontal laminations are visible in the top of 10 cm of the clay. This layer can be seen in the floors of both open pits. Although there are a number of coal seams of different thicknesses, only two coal seams called upper and lower seams, with an average thickness of 7 m, may be mined economically. They are separated by an interburden consisting of medium to dark grey dry to damp, weak to very weak clayey silt. It includes bedding apparent as light gray thin silt bands (see Fig. 3).

The overburden above the upper coal seam is approximately 80 m thick, and comprises greenish marls and brown siltstones overlain by a more competent capping of karstic limestone. Medium grey wet silty clay, firm to stiff marl, overlain by light brown, damp very weak siltstones, represent the lower part of the overburden, and form the benches above the upper coal seam. The greenish marls are very weak when dry, and break down to silty clay when exposed to free water. Light grey, strong, slightly weathered karstic limestones form the uppermost benches of the pits. The greenish marls and limestones belong to the Bicir formation. The limestones are used for surfacing benches to improve trafficability and for construction of the dragline bearing pads. The thickness of the Bicir formation ranges between 20 and 50 m.

Plio-Quaternary aged young basalts form the southern boundary of the South Pit. Quaternary alluvial deposits fill the valley along Balıklan stream to the west of the Central Pit (see Fig. 4).

The dip of bedding planes both in the Kalburcayiri and Bicir formations ranges between 4° and 9° towards the NW. The bottom clay, which conforms to the dip of coal seam, may dip in either a northwesterly or northeasterly direction into the Central Pit at angles ranging

from 4° to 6°. The plunge of the syncline axis in the Tertiary units is between 3° and 4° toward the NNW. Only very small faults are visible on the pit walls. However, borehole data obtained from MTA (1976) suggest the presence of three main normal faults shown in Fig. 4.

Climate

Hot and dry summers, and cold, rainy and/or snowy winters prevail throughout the province. According to the records between 1931 and 1980, and 1992 and 2002, from the nearest meteorological station 30 km from the operated open pits, rainfall generally falls in high intensity storms between January and May (Fig. 5a). The mean monthly rainfall ranges from 6 to 59.8 mm. Spring thaw usually occurs in late March and April and contributes much runoff and infiltration to slopes.

The comparison between the mean monthly precipitation from 1931 to 1980 and in 2001 (Fig. 5b) suggests that the precipitation in May 2001, before the spoil piles failed, is considerably higher than the mean precipitation for May. In addition, the cumulative precipitation to May 2001 was considerably higher than the average (Fig. 5c).

Site investigations

Description of spoil pile failures

In the early stages of the investigation, field work in the form of observations and surveying was carried out to deduce the basic characteristics of the large spoil pile failure (INS1) in the Central Pit (see Fig. 1a) and the small-scale failure (INS2) in the old outside dumping area (see Fig. 1b).

INS1 occurred on the evening of the 10 June 2001 in the central part of the inside dumping area of the Central Pit. Due to lack of monitoring studies before the failure, no information about the rate of the movement is available. Based on information from mine personnel, only few tension cracks behind the crest of the dump were noticed for the first time some weeks before the failure occurred. Prior to the failure, the dump height was 40 m at the pit edge and 115 m at the crest (Fig. 6). The overall slope of the dump was 12° and there was a 65 m wide berm at 1,584 m elevation, 15 m below the dump crest. The distance between the highwall and the back slope of the failure face was about 600 m. The failure involved 20,000,000 m³ spoil material and covered an area of approximately 0.3 km².

Observations and the inclination of the floor showed clear evidence of the mode of failure. At the back of the failure, there was a well defined scarp where failed

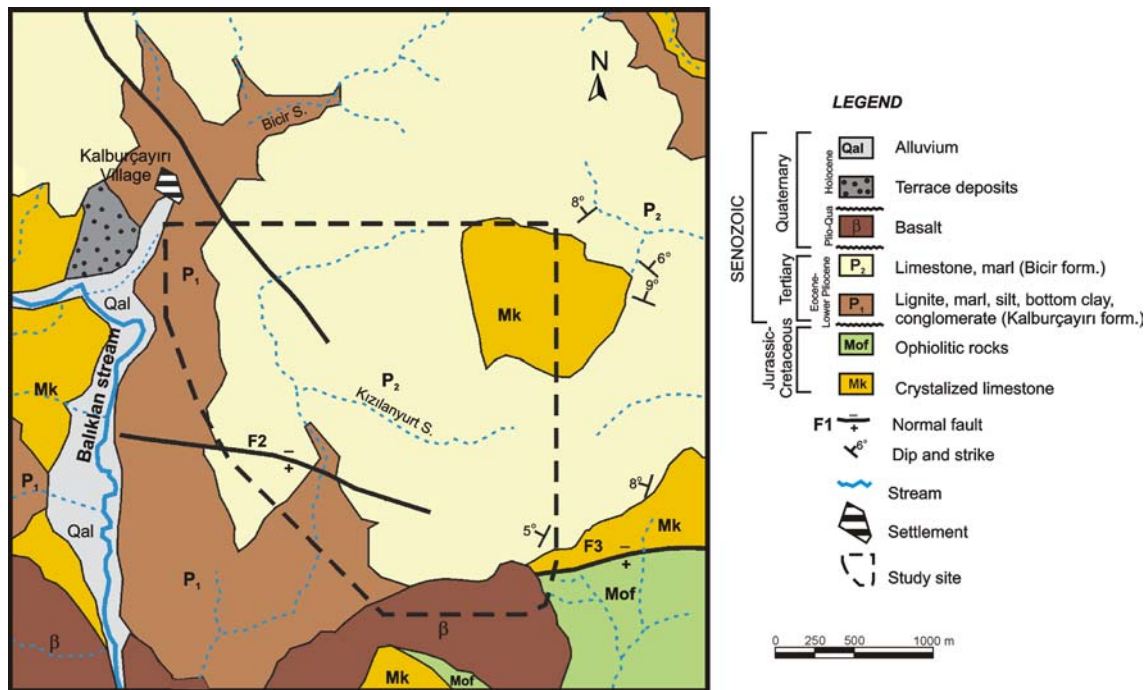


Fig. 4 Geological map of the study site (rearranged from MTA, 1976)

material at the base of the failure has dropped lower in elevation than material at the front (Fig. 7a). Some backward-tilted sections of the uppermost spoil benches moved down along this surface as seen in Fig. 7a. This would suggest that circular failure (rotational movement) initiated the failure from the back of the dump where the dump height was at a maximum. The dragline spoil piles moved roughly horizontally, with no discernible change to their conical shape (Fig. 7b). This suggests that the toe of the dump underwent a translational movement parallel to the base of the pit floor. A discrete interface between the failed dump and the area to the west, which did not fail, was evident. The contour plan of the pit floor indicates that the failed dump lies above a syncline-shaped structure with limbs dipping at 4° and 6° to the east and west, respectively, and with a plunge of 3° – 4° towards the highwall (Fig. 7c). These observations suggest a combined failure consisting of a circular sliding surface passing through the spoil material at the upper part of the dump and a planar surface along the interface between the bottom clay (floor) and the interburden dragline spoil piles (Fig. 8). The floor geometry facilitated movement of the spoil material towards the mining face and is possibly one of the most important contributors to the instability.

A small and local instability (INS2) also occurred in 2002, during the site investigation stage of this study, at the old outside dumping area, which is located on natural slopes dipping to the Balıklıan stream (see Fig. 1b). Some tension cracks 5–10 cm wide and settlements of

about 40 to 50 cm on the road connecting the Central Pit to the recreation area were observed. In addition, heave and seepage at the toe of the spoil pile were evident. However, the movement did not extend to the haul road and did not affect mining operations. Observations and the natural topography, underlying the dump, indicated that the failure occurred along a spiral surface passing through the spoil material in the upper benches and following the topographical surface at the base of the spoil pile.

Groundwater considerations

Because no previous information was available, the assessment of hydrogeological conditions in the spoil piles was based on drill-hole records, and general observations carried out in both pits following the instability INS1. The overburden is generally wet. Dewatering by the mining company effectively removed the free water in the karstic limestone. However, due to their low permeability, the lower overburden units remained unaffected by the dewatering. A water flow was observed on a bench on the eastern slope of the South Pit in the summer of 2002 (location 1 in Fig. 9). This flow is collected in small pools and 150 – 160 m^3 of the collected water from these pools is used in wetting the haul roads in dry seasons. In addition, water accumulated on the bottom clay between the highwall and dragline spoil piles of the South Pit, either by infiltration

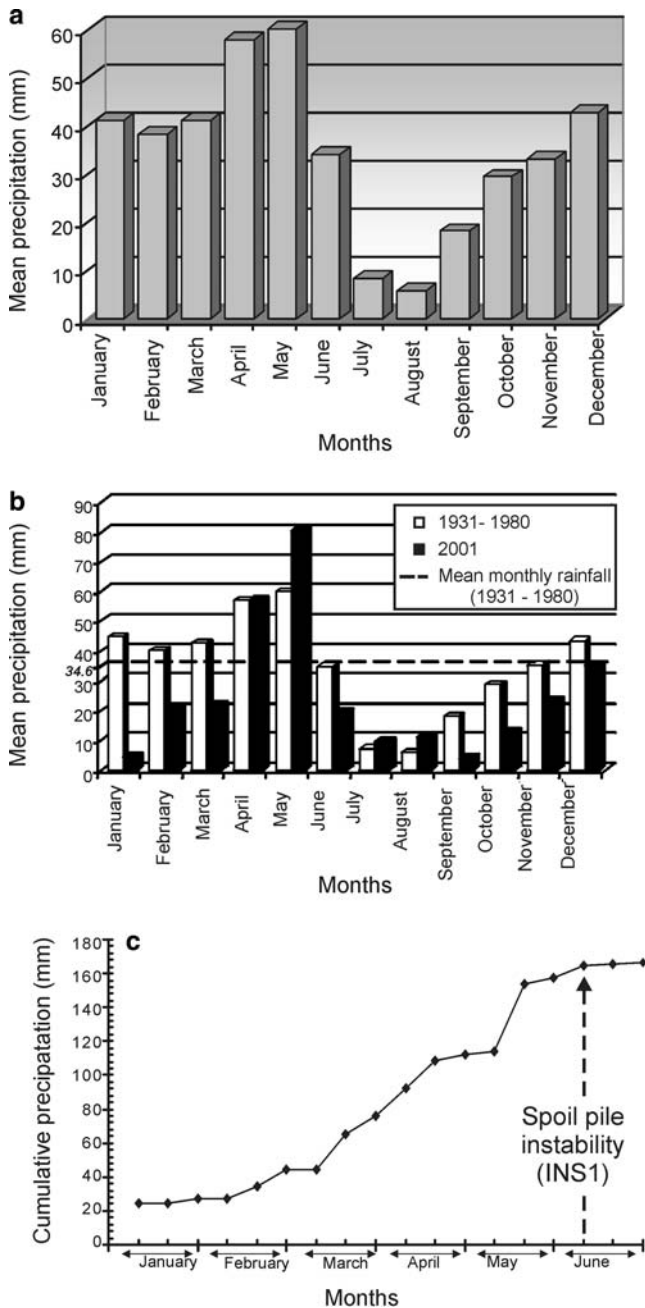


Fig. 5 **a** Histogram showing the mean monthly precipitation between 1931–1980 and 1992–2002, **b** comparison of mean monthly precipitation between 1931 and 1980 and the year of 2001, **c** cumulative precipitation for the first 6 months of 2001 and date of spoil instability INS1

or surface runoff (location 2 in Fig. 9). In addition to a few seepage locations, there also exist some water pools from the east to the west in the area of INS1 at the Central Pit (see Fig. 9). These observations suggested two scenarios. Firstly, as a result of the depositional structure of the spoil, some quantities of water may seep

down through discrete zones in the spoil to the base. Secondly, the water accumulated at the base of the South Pit (location 2 in Fig. 9) may flow from the floor below the spoil dumps between the two pits towards the spoil piles at the Central Pit.

The above-mentioned scenarios were investigated by drill-holes. Eight holes were drilled in the spoil pile at the Central Pit between the upper failure surface of INS1 and the toe of the piles, using a blast hole drilling machine capable of drilling capacity to 28 m depth. Their locations, which were decided based on the capacity of the drilling machine, ease of access and the locations of water pools, are shown in Fig. 9. Except for drill-holes D1, D5 and D7, in which no water was observed, the depth to the water from the surface measured in the remaining holes ranged between 5 and 17 m. These levels indicate the presence of standing water in the spoil piles above the spoil-floor contact, particularly at isolated areas.

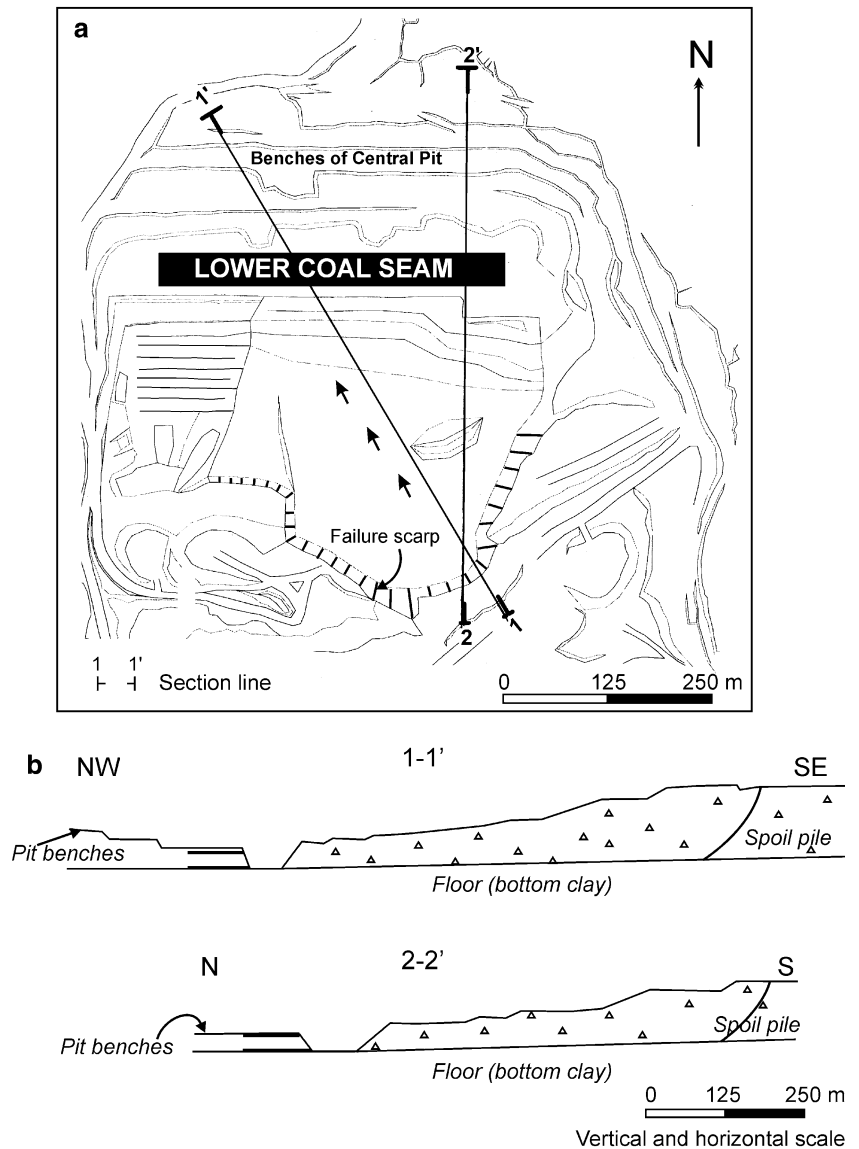
Based on the above-mentioned assessments, it was concluded that most of the water would appear to be held within the overburden material in the dump either from rainfall or groundwater held within the wet overburden dump material.

Assessment of deformations by monitoring data

Simple observations by the mining company after the failure indicated that a slow movement behind the crest of the failure INS1 might be occurring in addition to the the small-scale spoil pile instability, INS2, initiated during this study. Hence, a slope monitoring study was conducted to determine if there were any patterns that might be used to assess the character of the movement after the INS1 failure and to define the failure geometry and mechanism of INS2. During this study, sophisticated monitoring devices, such as inclinometers and extensometers were not available. Therefore, monitoring was conducted at the surface by means of electronic distance measuring (EDM) equipment, 1200 informatic theodolite and D14 distomat. At the beginning, reflectors fixed on rods were established at 43 monitoring stations in the Central pit and the area of INS2. However, due to the loss of some stations as a result of mining activities, monitoring was continued using 34 stations. The monitoring was implemented in August 2001 and ceased in April 2003. The locations of the monitoring target stations are shown in Fig. 10a. The coordinates and the elevation of each target station, from which movement vectors between successive readings can be calculated, were recorded.

The cumulative displacements of stations 13, 14, 15, 17, 36, 37, 43 and 47, which are situated at the back of the instability INS1, ranged between 191 and 639 mm (see Fig. 10a). These stations were moving downwards

Fig. 6 **a** Simplified plan of instability INS1 and **b** typical cross-sections of spoil pile geometry deduced from surveying before and after the instability



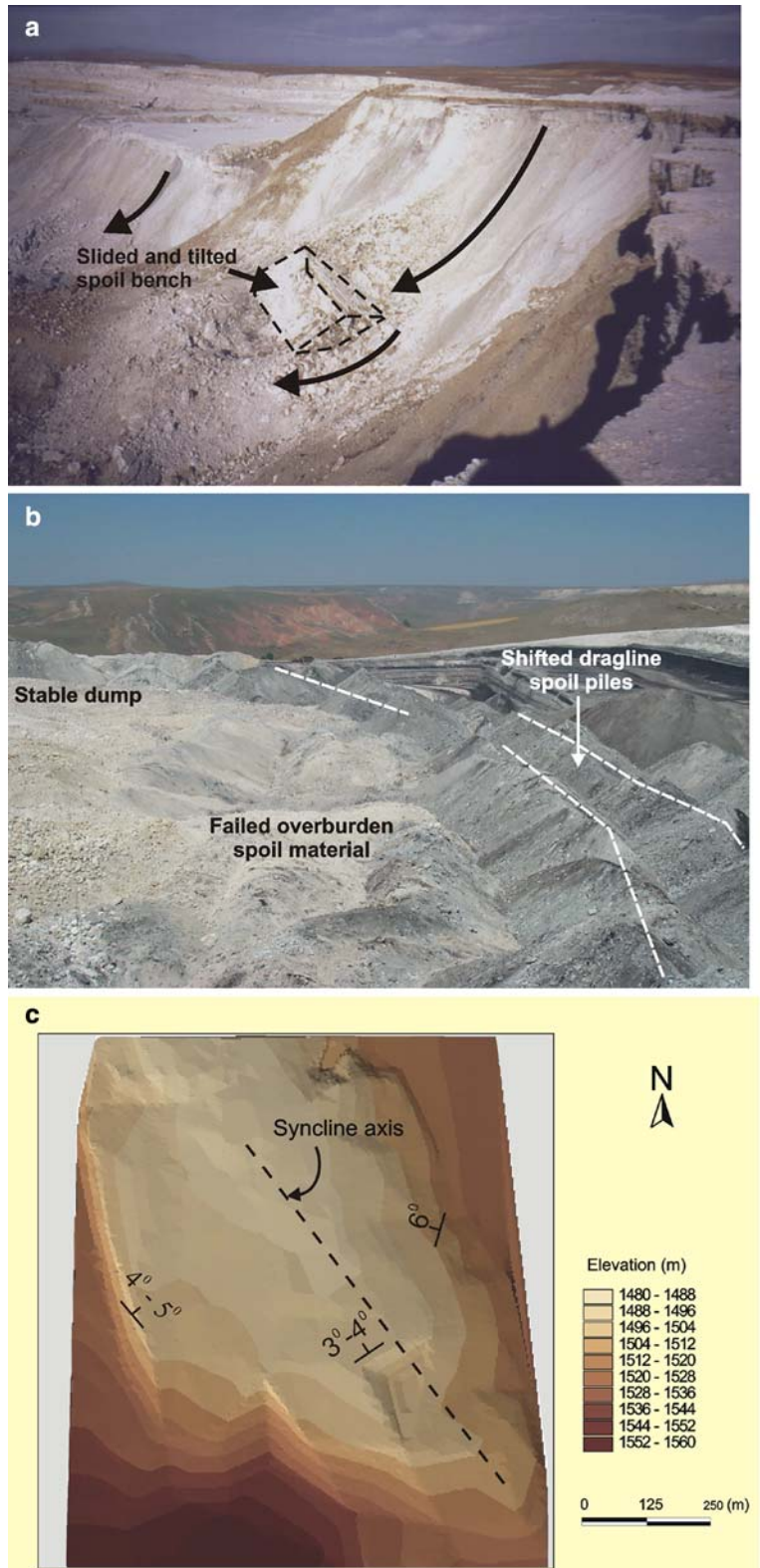
at plunges (deviation from horizontal plane) of 60° – 75° . Magnitudes of movements at stations 15 and 37 were greater than those at other stations mentioned due to the movement of the suspended spoil blocks located at the crest of the failure and bounded by tension cracks and the failure scarp (Fig. 10b). Greater cumulative displacements at stations 40, 42 and 44, which are located at the lower part of the instability, resulted from the compaction of spoil material dumped to provide a buttress to contain the failed material. A typical example of time versus cumulative displacement from one of the stations established in the area of INS1 is depicted in Fig. 10c. It is clear from the graph that displacements in the vertical direction generally control the movement after the failure throughout the monitoring period. All time versus cumulative displacement plots from the

target stations indicate that displacements clearly tend to decrease after February 2002.

Six cross sections from different parts of the failed spoil pile were prepared and the resultant movement vectors are shown on these cross sections (Fig. 11). The directions of the movement vectors shown in Fig. 11 confirm the above assessments. Therefore, it can be concluded that the large-scale spoil failure (INS1) is not still active, and the ongoing deformations are mainly due to the compaction of the spoil material. In addition, movement of the individual spoil blocks, which rest on the back scarp of the failure surface, also contributes to the deformations measured at the stations close to the crest.

Monitoring data taken from six stations established in the local instability at the outside dumping area

Fig. 7 **a** Scarp (circular failure) of instability INS1, **b** horizontal dislocation of dragline spoil piles, and **c** contour map of the floor in the Central Pit



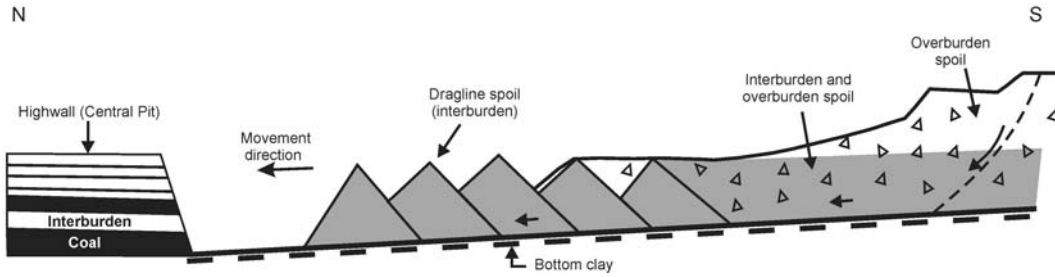
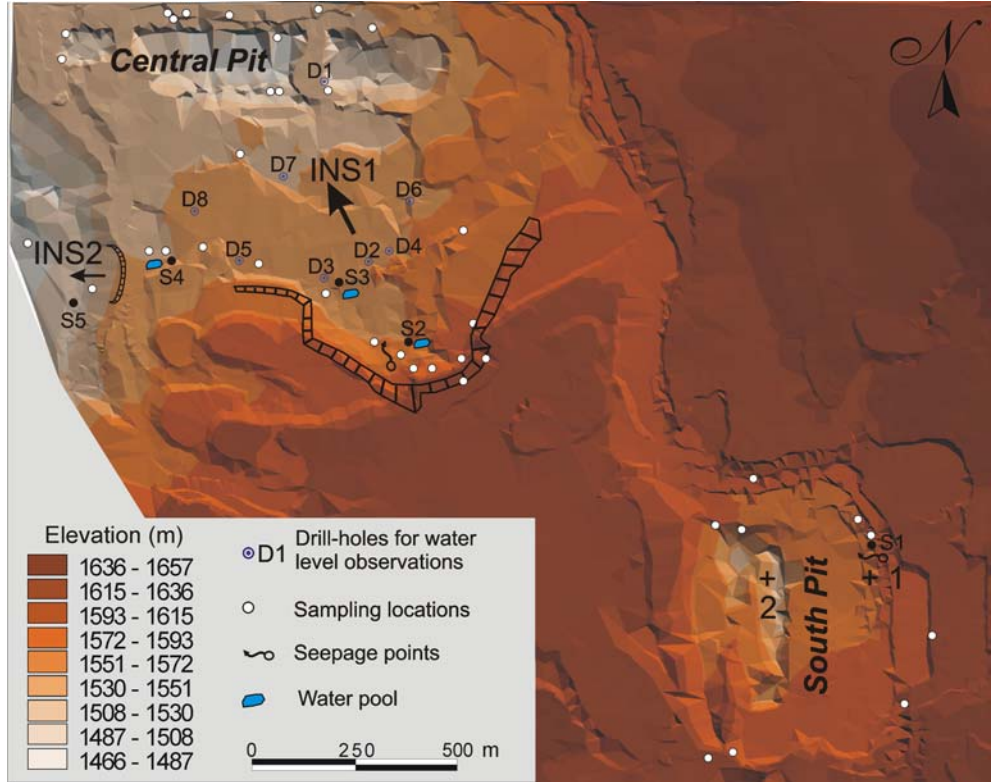


Fig. 8 Section through the spoil dump illustrating failure mechanism for instability INS1 (not-to-scale)

Fig. 9 Locations of the hydro-geological investigations involving water-well drilling, water sampling and observations



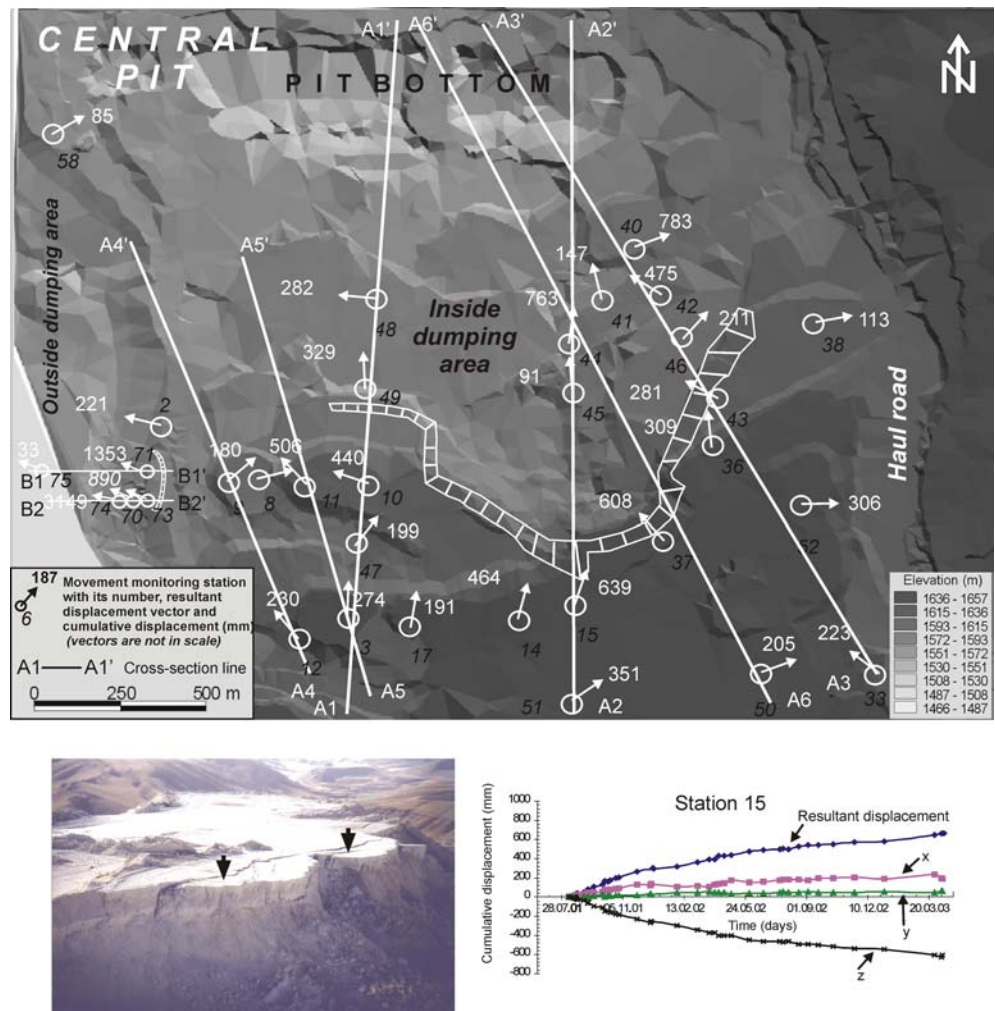
(INS2) were also evaluated and the resultant movement vectors are shown in Fig. 12a. The position of the tension cracks suggest that this movement was limited by the haul road to the east. However, based on the plunges of stations 71 and 73, a considerable amount of vertical deformation occurred on the road connecting the pit to the recreation area (70° and 79°; see Fig. 12a). As can be seen from Fig. 12a, direction of the resultant movement vectors indicate that the failure has probably initiated along a circular surface through the old spoil material near the road to the recreation area and then passed through the spoil or along the natural topographical surface beneath the dumps. The movement vector at station 75 displays an upward direction, and therefore, the location of this station can possibly be considered as the toe of the failure (see Fig. 12a). An example time

versus cumulative displacement graph from a station shown in Fig. 12b suggests that the movement accelerated, particularly in March 2003, and failure was completed at the end of March 2003.

Characterization of materials

Sampling of both overburden and dragline spoils, floor material (bottom clay) and the unit forming the natural slopes of the outside dumping area was carried out, despite the difficulties caused by the presence of blocky rock fragments within the zone of instability and sliding surface. In addition, the in-situ unit weight of the spoil material was determined in two trial trenches. Specimen cutters, 100 mm square by 300 mm thick, were utilized

Fig. 10 a Locations of movement monitoring stations and resultant displacement vectors, **b** a suspended spoil block on the backscarp of INS1, and **c** a typical cumulative displacement versus time plot.



for undisturbed sampling. Samples from the floor were recovered with an orientation parallel to the displacement. Throughout the laboratory tests, the ASTM (1994) standards were employed.

Based on X-ray diffraction analyses, clay minerals dominate the overburden spoil, bottom clay and in-situ material forming the natural slopes in the outside dumping area. Kaolinite is the chief clay mineral (Table 1). The in-situ unit weight of the overburden spoil and dragline spoil materials were determined in two trial trenches as 16.3 and 15.1 kN/m³, respectively. However, the values of unit weight were also determined from 35 undisturbed samples taken by metal specimen cutters (Table 1). Due to more compaction effects, the unit weight of the overburden spoil pile material dumped by trucks is greater than that of the dragline spoil material.

Grain size analyses were conducted on 11 samples after removing the large particles that could not be analyzed by standard sieves and do not play an important role in the stability of piles. The results (Table 1)

indicated that except for the interburden spoil material, the fines content dominates in all materials. The dominant grain size in all materials was silt-sized. This is probably due to breakdown of the spoil materials by hauling, dumping and truck traffic. This situation reveals that the behavior of the finer fraction in the dumps dominates the overall behavior.

The moisture content of the spoil materials ranges between 30.7 and 49.7%, indicating that they were wet. Atterberg limits of the samples of spoil fines, bottom clay and natural slope forming material are tabulated in Table 1. Except for those samples from the interburden material, the majority had liquid limit values exceeding 50%. The overburden and interburden spoil materials are classified as CL and CH, and GC according to the Unified Soil Classification, indicating silty clay, high plasticity clay and gravel-sand-silt, respectively.

It was considered essential that the anticipated full range of in-situ normal stresses acting on the sliding surfaces throughout the investigated piles be duplicated in the laboratory in order to obtain reliable results from

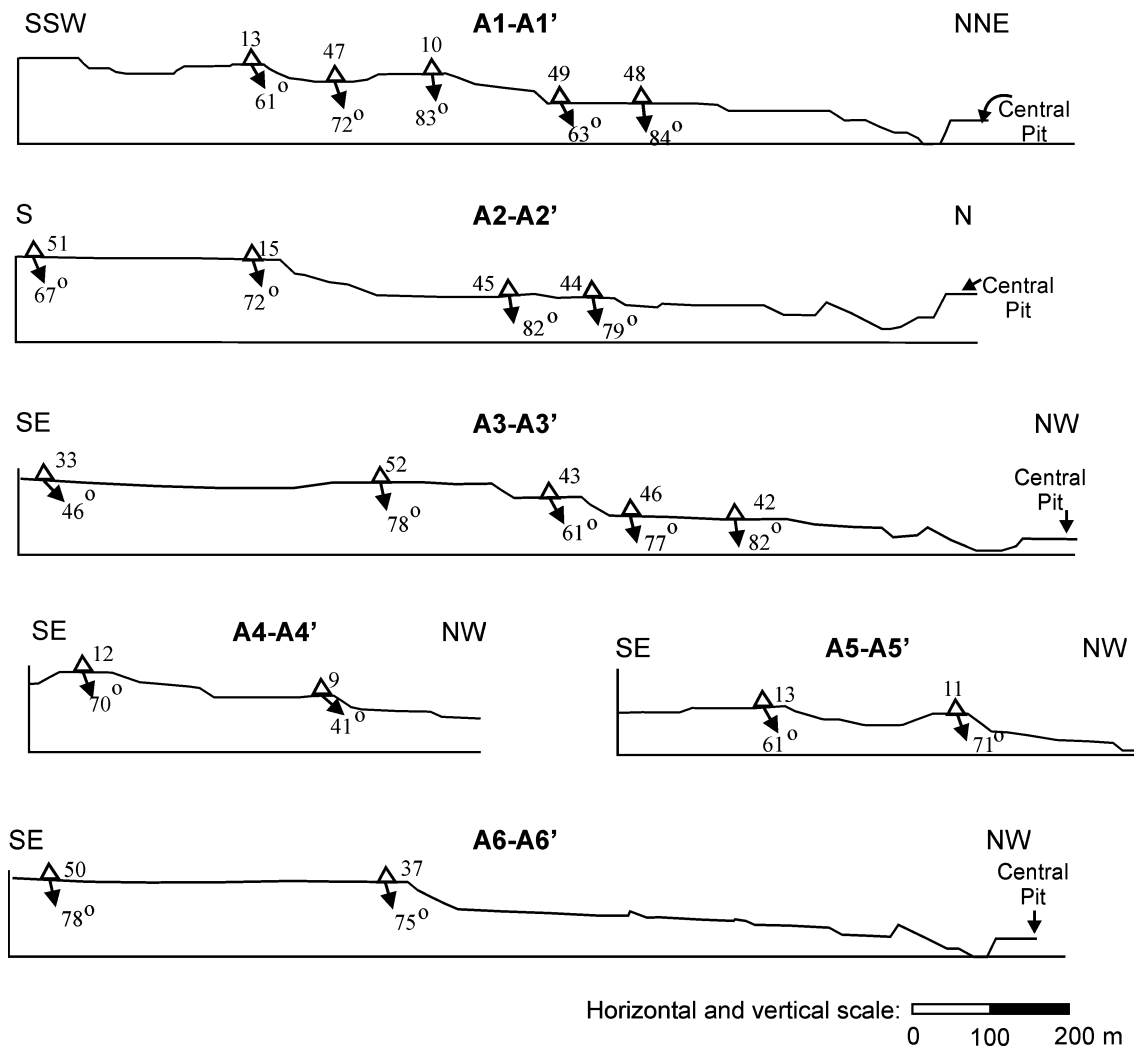


Fig. 11 Cross-sections from instability INS1 showing resultant movement vectors with their plunges.

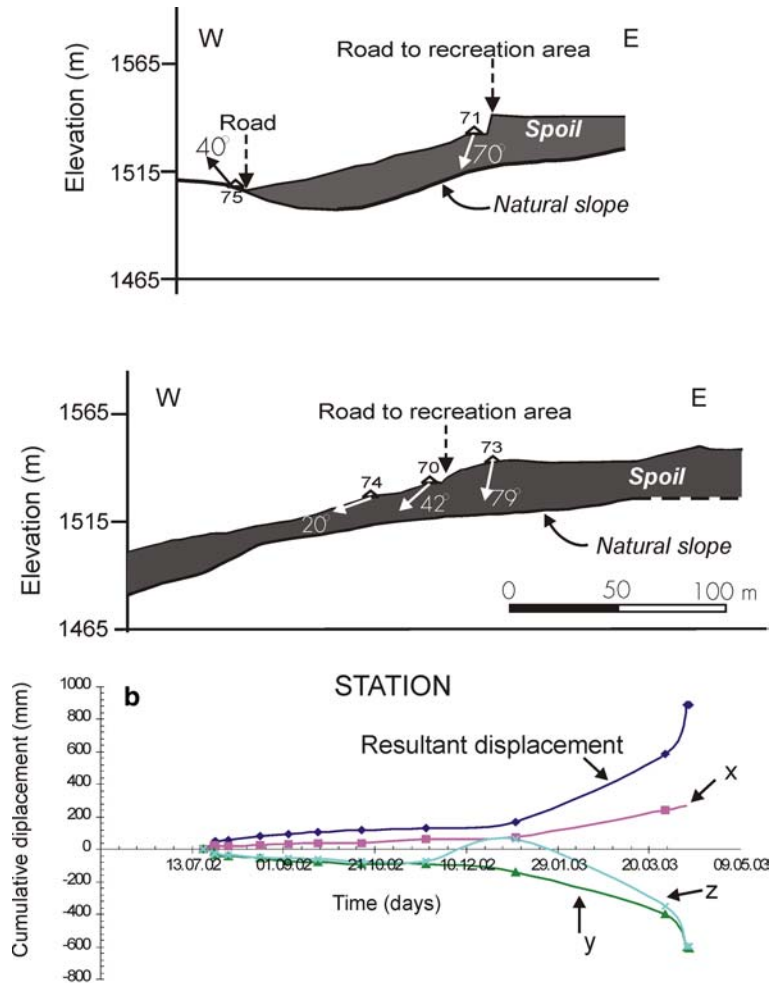
the shear strength determinations. All of the samples, therefore, were tested at normal loads, consistent with field loading conditions. A motorized direct-residual shear test device with strain control and shear box assembly was used, and the samples were tested under consolidated-drained conditions. The materials sampled were grouped as overburden consisting of beige colored silty soil and green marl, which is transformed into a clay-like soil after dumping, and interburden (dragline spoil pile), bottom clay and natural slope forming material.

Direct shear tests were carried out on 17 test series consisting of a minimum of three samples, to achieve representative failure envelopes. A total of 55 specimens prepared from the undisturbed spoil materials, bottom clay and natural slope forming material were tested. The shear strengths of the weak interfaces between the dragline spoil and the bottom clay, and the spoil and

natural material forming the slopes of the outside dumping area were also determined. For this purpose, undisturbed samples from the bottom clay and/or natural material were placed into the lower half of the shear box and dragline spoil material (interburden) and/or spoil material from instability INS2 were placed in the upper half. Tests were carried out at a very slow shear strain rate (0.05 mm/s) to allow drainage by cycles of shear reversals and normal loads corresponding to 50–850 kPa were applied representing the expected normal stresses at different parts of the spoil piles.

Generally, the peak shear strength for the beige silty overburden material, which dominates in the spoil piles, was reached after a few millimeters of displacement, particularly at low normal stresses. This behavior was also observed for the other materials tested. Coal measure spoil materials are generally considered to behave as frictional materials (Thompson and Rodin, 1972).

Fig. 12 a Resultant movement vectors shown on the cross-sections, and **b** a typical cumulative displacement versus time plot from INS2.



However, Taylor (1973), who studied the compositional and geotechnical characteristics of an old colliery spoil heap, suggested that there was more than an 80% probability of a positive cohesion intercept. In the literature, some investigators suggested that shear strength of spoil piles of blasted, excavated and dumped weak overburden is better represented by a linear (Mohr-Coulomb) failure envelope (Richards 1982; Williams and Walker 1985; Okagbue 1987; Ulusay et al. 1995, 1996). In addition, some investigators suggested that the shear strength of more blocky spoil piles is better represented by power curve relations (Thompson and Rodin 1972; Barton and Kjarnesli 1981; Stead and Singh 1989). Considering these suggestions, in addition to the linear Mohr-Coulomb's criterion, the relationship $\tau = A\sigma^B$ (power curve regression) was also tested. To obtain the generalized failure envelope for each material, plots of individual test series were transferred to a single plot. Generalized failure envelopes derived from both linear and power curve relationships yielded very high correlation coefficients ($r = 0.96\text{--}0.99$). It is also noted that there is no significant difference between the linear

and power-law envelopes of both the peak and residual shear strengths for the normal stresses expected in the spoil piles. Therefore, effective peak and residual cohesion and friction angles based on linear failure envelopes (Table 2) were adopted in the stability analyses. It is evident from Table 2 that the shear strength of the interface between the bottom clay and dragline spoil is considerably lower than that of the bottom clay, indicating that this interface is the critical surface for pile stability. A similar conclusion can also be made for the interface between the dumps and the natural topographical surface at the outside dumping area.

The elasticity modulus of the spoil material to be used as an input parameter in numerical analyses was also determined. For this purpose, two remoulded triaxial test specimens of 38 mm diameter and 90 mm height were prepared from silty material (BR), which is dominant in the overburden spoil, and tested under consolidated-drained conditions. The loading rate was 0.05 mm/s and cell pressures of 150 and 250 kPa were applied. The tangent modulus (E_{50}) of the specimens was

Table 1 Material characteristics

Mineral type (%)									
Material	Main minerals					Clay minerals			
	Mica	Quartz	Calcite	Dolomite	Clay	Smectite	Illite	Kaolinite	Attapulgite
X-ray diffraction analysis results									
GM	23.6	1.7	30.4	1.8	42.5	20.4	–	22.1	–
S	13.1	7.5	3.1	–	76.3	38.2	16.0	22.1	–
BC	–	2.8	16.2	0.8	80.2	–	57.0	8.4	14.8
DS	–	3.8	96.2	–	11.3	–	–	–	–
NSM	14.8	2.3	25.7	2.2	55.0	22.6	–	32.4	–
Unit weight (kN/m ³)									
	S 16.9–19.4 (17.6)		GM 17–17.5 (17.3)		DS 15.8–16.2 (16)		BC 18.2–18.5 (18.4)		NSM 18.2–18.6 (18.4)
Physical and index properties									
Grain size distribution									
Gravel (%)	1–20		7–20		38		0		4
Sand (%)	6–35		4–17		14		4		10
Silt (%)	33–53		46–48		39		35		33
Clay (%)	10–57		17–41		9		61		53
Moisture content (%)									
	31.6		49.7		30.7		39.1		30.4
Atterberg limits									
LL (%)	37–49 (43.5)		63–72 (66.4)		35		68–76 (73.2)		59–65 (62.3)
PL (%)	18–24 (21)		26–30 (27.8)		24		21–27 (23.5)		21–26 (23)
PI (%)	17–26 (22.5)		36–43 (38.6)		11		45–53 (49.7)		37–41 (39.3)
Unified Soil Classification	CL		CH		GC		CH		CH

Numbers given in parantheses are the mean values

GM green marl; S silty material (overburden); BC bottom clay; DS dragline spoil; NSM natural slope forming material in INS2

determined as 10.3 and 8.3 MPa, at 150 and 250 kPa, respectively.

Stability evaluations

In order to assess the failure mechanisms, and to estimate pore water conditions at the time of failure, back-

analysis using the two-dimensional limit equilibrium technique and numerical modeling were performed for both instabilities. As discussed earlier, the spoil pile failures involved displacements through the spoil itself and along the interface between the floor and interburden spoil piles. Accordingly, limit equilibrium back-analyses were performed on two sections derived from the plans of instabilities INS1 and INS2, using Janbu's

Table 2 Shear strength parameters derived from generalized failure envelopes

Material	Peak shear strength		Residual shear strength	
	c_p (kPa)	ϕ_p (°)	c_r (kPa)	ϕ_r (°)
S	16–26	31.1–32.4	3.3–11.7	26.2–29.8
GM	25.3–34.4	33–33.8	2.5–5.9	32.5–32.7
DS	17.5	30.5	10.1	23.6
BC	46.5–65.5	19.4–23.7	11.5–22.1	13.7–16.3
DS/BC	7.9–14.8	22.2–23.8	1.4–8.9	10.5–13.8
NSM	47.1	14.2	32.3	11.2
OSM	21.9	28.8	11.9	25.4
OSM/NSP	12.4	29	4.9	27.5

GM green marl; S silty material (overburden); BC bottom clay; DS dragline spoil; NSM natural slope forming material in INS2; DS/BC Interface between spoil and bottom clay; OSM spoil material at the outside dumping area; OSM/NSP interface between the spoil material and the natural slope

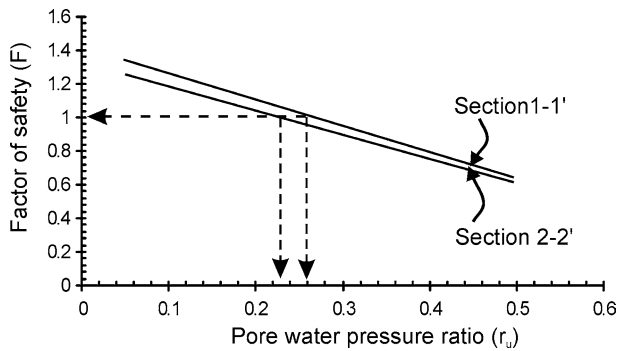


Fig. 13 Variation of factor of safety with pore water pressure ratio for INS1.

method of stability analysis (Janbu 1973). In the analyses, a slope stability program Slope 8 (1999) was utilized. For the numerical analyses a computer code Plaxis (1998 v. 7.2), based on FEM, was used to simulate only INS1. In the FEM analyses an elastic-perfectly plastic constitutive model incorporating the Mohr-Coulomb yield criterion was employed. A “ c - ϕ reduction procedure” embodied within Plaxis was also used to estimate the factor of safety of the slope. Assumptions made in

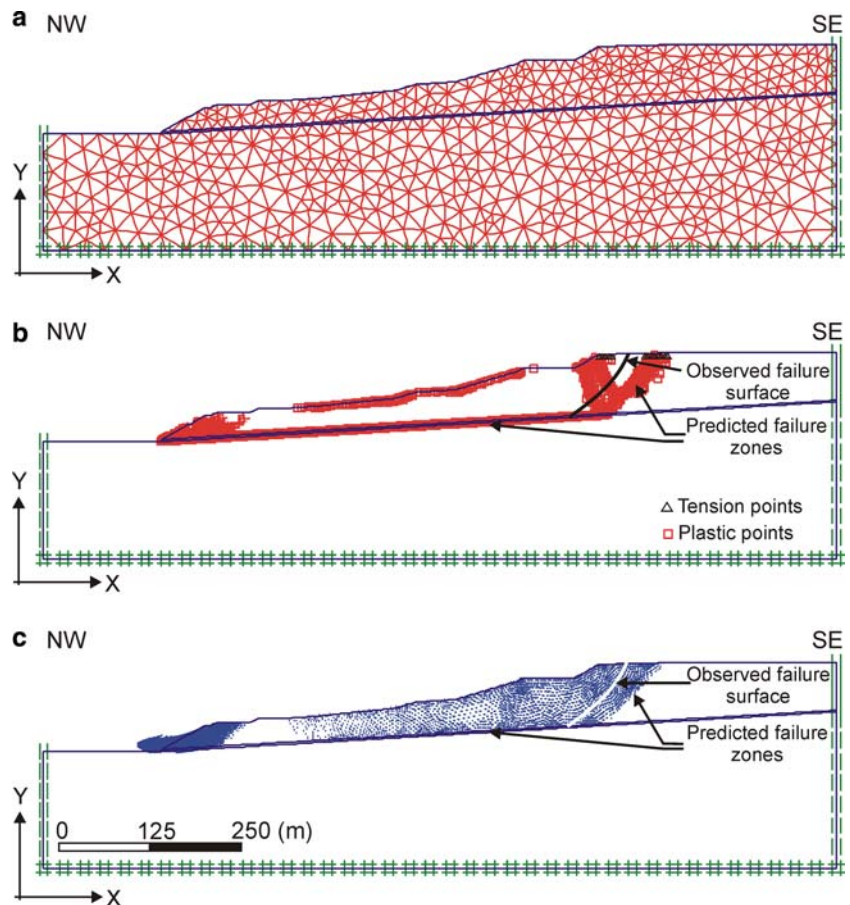
the analyses and the results are discussed in the following paragraphs.

Evaluation of the failure (INS1) in the Central Pit

In the back-analysis of INS1 instability, the failure mechanism depicted in Fig. 8 was considered. In addition, based on the sharp decreases in shear strength post-peak for the materials investigated, it was considered to be realistic to assume that the spoil pile materials and weak interface between the floor and the dumps exhibited shear strengths at or approaching the residual values at the time of failure. Therefore, the minimum values of residual shear strength parameters of the overburden spoil material and bottom clay given in Table 2 were utilized in the analyses. Considering that the beige colored silty material is the dominant overburden material in the spoils dumped by trucks, its residual shear strength parameters were used to represent the shear strength of the circular part of the failure surface.

Hydrogeological investigations indicated that there exist standing water levels in the spoil piles. However, it is difficult to estimate a particular groundwater level. Although the residual shear strength of the interface

Fig. 14. **a** Finite element configuration and boundary conditions of the model along cross-section 1-1', **b** distribution of yield points and **c** calculated nodal displacements with the observed failure surface for instability INS1



between the dragline spoil piles and floor and of the overburden spoil material are low, water had to be introduced into analyses to initiate the failure. Therefore, a pore water pressure coefficient (r_u), which is the ratio of the pore pressure to the soil pressure at any point in the layer, was employed.

Back-analyses were carried out to assess the sensitivity of the spoil piles to variations in pore water pressure and to estimate the r_u values satisfying the limit equilibrium condition for the two cross-sections from the failure shown in Fig. 6. The results shown in Fig. 13 suggest that pore water pressure ratios satisfying the limit equilibrium condition are 0.26 and 0.23 for cross-sections 1-1' and 2-2', respectively. These r_u values are equivalent to a material that is approximately 45–50% submerged. It should also be remembered that, as discussed in hydrogeology section, heavy rainfall occurred about 1 month before the failure (see Fig. 5). Infiltration of the rainfall into the spoil materials would likely have led to an increase in pore water pressure just prior to the failure. In addition, the floor geometry promoted groundwater flow towards the mining face, reducing the shear strength of the interface between the floor and the spoil piles. Both these effects would contribute to instability.

Numerical analysis of INS1 was carried out on cross-section 1-1'. The geometry, boundary conditions, and finite-element mesh used in the numerical analysis are depicted in Fig. 14a. Nodal displacements were constrained to zero at the vertical boundaries of the mesh. In the analysis, r_u was taken as 0.26, which satisfied the limit equilibrium condition for the cross-section considered. Figures 14b and c display the yield points and displacement vectors, respectively, together with the observed sliding surface. As can be seen from Figs. 14b and c, the estimated failure zone from the FEM analysis is very close to the observed failure surface. In other words, plastic zones appear along the circular failure surface and the interface between the floor and the spoil piles. In addition, tension zones are in good agreement with the locations of the tension cracks observed at the crest of the instability. However, another plastic zone appears at the toe zone of the instability (Figs. 14b, c), indicating a movement at the toe of the dump. Based on the information from mine personnel, no separate movement was observed at the toe zone. This contradiction can be explained by two possibilities. Firstly, due

to fast rate of failure, a local movement at the toe could not have been recognized. Secondly, the r_u value used in the numerical analysis applies to the entire spoil, but the toe berm is relatively small, resulting in toe movement.

Evaluation of the local instability (INS2)

Considering field observations and movement monitoring data, a back-analysis of the local instability (INS2) was carried out. In the analysis, Janbu's method and the residual shear strength parameters of the spoil and natural slope forming materials, and their interface (see Table 2) were utilized. Due to the presence of water flow in the spoil, factors of safety for various r_u values were calculated. As can be seen from Table 3, even for drained piles ($r_u = 0$) the factor of safety is slightly lower than unity, indicating that the shear strength parameters reduced to residual values at the time of failure. In other words, a weak basal surface beneath the dump and isolated water zones in this old pile are the main contributing factors to instability.

Conclusions and recommendations

Observations, monitoring data and back-analysis using the 2-D limit equilibrium method and numerical techniques suggest that a compound sliding failure mechanism is realistic for the spoil pile failure in the pit. Movement of the spoil piles was initiated by the softening of moisture sensitive material at the base of the spoil and the cracking of spoil material due to settlement and compaction movements. In both failures, the investigated sliding surfaces are composed of a circular surface passing through the spoil itself and a planar surface along the weak interface between the floor strata (bottom clay) and the dumps. The failure surfaces were also confirmed by the results of deterministic and numerical analyses. In addition, adverse dips of the floor strata, on which dumping was carried out, is one of the factors promoting the initiation of movements into the unsupported void. However, because the floor dip changes to the south (i.e. opposite the spoil pile faces) beyond the existing highwall, this change may positively influence the stability of the spoil piles.

Water level measurements and moisture content determinations suggest that water would appear to be held within the overburden material in the dump, either from precipitation or as groundwater held within the wet overburden spoil material. Stability analyses showed that an average pore water pressure ratio of about 0.25 satisfies the limiting equilibrium condition indicating

Table 3 Variation of factor of safety (F) with pore water pressure ratio (r_u) for INS2

r_u	F
0.00	0.96
0.05	0.93
0.10	0.89
0.15	0.86

that movement is likely. In addition, unexpected amount of rainfall that occurred one month prior to the large failure (INS1) may be considered as another triggering factor. To avoid the reoccurrence of a similar event in the future, and to ensure the long term safety, movement

monitoring studies should be continued both in the Central and South Pits.

Acknowledgements The authors wish to acknowledge the cooperation and valuable support of the mining company and mine personnel. They would also like to thank Nihat Sinan Isık (Gazi University) for his valuable contributions in numerical analyses.

References

- ASTM (American Society for Testing and Materials) (1994) Annual book of ASTM standards—oil and rock, building stones, Section 4, Construction. V.04.08, ASTM Publication
- Barton NR, Kjarnesli B (1981) Shear strength of rockfill. *ASCE J Geotech Eng Div* 107:873–891
- Bowman PM, Gilchrist HG (1978) Waste dump instability and its operational impact for a Canadian Plains lignite mine. In: Proceedings of the international symposium on stability in coal mining. Vancouver, British Columbia, Canada, pp 381–394
- Janbu N (1973) Slope stability computation. Embankment dam engineering, Cassagrande volume. In: Hirschfield RC, Poulos SJ (eds) Wiley, New York, pp 47–86
- MTA (1976) Feasibility report for a coal field in Central Anatolia. General Directorate of Mineral Research and Exploration of Turkey (unpublished report in Turkish)
- Plaxis (1998) Finite element code for soil and rock analyses. Balkema, Netherlands
- Okagbue CO (1987) Stability of waste spoils in an area strip mine - geological and geotechnical considerations. *Earth Surf Processes Landforms* 12:189–300
- Richards BG (1982) The finite element analysis of mine spoil slopes using slip elements to simulate strain softening yield behavior. *Civil Eng Trans* 24(1):69–76
- Richards BG, Coulthard MA, Toh CT (1981) Analysis of slope stability at Goonyella Mine. *Can Geotech J* 18:179–194
- Slope 8 (1999) GeoStru Software version 8.0 revision 52 User's Manual. GeoStruct Enterprise, Italy
- Speck RC, Huang SL, Kroeger EB (1993) Large-scale slope movements and their affect on spoil-pile stability in Interior Alaska. *Int J Surface Min Recl* 7(4):161–166
- Stead D, Singh R (1989) Loosewall stability in United Kingdom surface coal mines. *Can Geotech J* 26:235–245
- Taylor RK (1973) Compositional and geotechnical characteristics of a 100-year-old colliery spoil heap. *Trans Min Metall* 82(784):A1–A14
- Thompson MG, Rodin S (1972) Colliery spoil tips - after Aberfan. *Inst Civil Eng* 7522:60
- Ulusay R, Arıkan F, Yöleri MF, Çağlan D (1995) Engineering geological characterization of coal mine waste material and an evaluation in the context of back - analysis of spoil pile instabilities in a strip mine, SW Turkey. *Eng Geol* 40:77–101
- Ulusay R, Çağlan D, Arıkan F, Yöleri MF (1996) Characteristics of biplanar wedge spoil pile instabilities and methods to improve stability. *Can Geotech J* 33(1):58–79
- Williams DJ, Walker LK (1985) Laboratory and field strength of mine waste rock. *Civil Eng Tran* 27(3):299–304